Title

18F-FDOPA PET and MRI characteristics correlate with degree of malignancy and predict survival in treatment-naïve gliomas: a cross-sectional study

Journal

Journal of Neuro-Oncology, 139(2)

ISSN

0167-594X

Authors

Patel, Chirag B

Fazzari, Elisa

Chakhoyan, Ararat

et al.

Publication Date

2018-09-01

DOI

10.1007/s11060-018-2877-6

Peer reviewed

HHS Public Access

Author manuscript

J Neurooncol. Author manuscript; available in PMC 2019 September 01.

Published in final edited form as:

J Neurooncol. 2018 September ; 139(2): 399–409. doi:10.1007/s11060-018-2877-6.

^{18}F-FDOPA PET and MRI characteristics correlate with degree of malignancy and predict survival in treatment-naïve gliomas: a cross-sectional study

Chirag B. Patel, MD, PhD[1,2,*], **Elisa Fazzari**[1,2,*], **Ararat Chakhoyan, PhD**[3,4,*], **Jingwen Yao, MS**[3,4], **Catalina Raymond, MS**[3,4], **Huytram Nguyen, BS**[1,2], **Jasmine Manoukian, BS**[1,2], **Nhung Nguyen**[1,2], **Whitney Pope, MD, PhD**[3,4], **Timothy F. Cloughesy, MD**[1,2], **Phioanh L. Nghiemphu, MD**[1,2], **Johannes Czernin, MD**[5], **Albert Lai, MD, PhD**[1,2], and **Benjamin M. Ellingson, PhD**[2,3,4,#]

[1]Department of Neurology, David Geffen School of Medicine, University of California, Los Angeles, Los Angeles, CA

[2]UCLA Neuro-Oncology Program, David Geffen School of Medicine, University of California Los Angeles, Los Angeles, CA

[3]UCLA Brain Tumor Imaging Laboratory (BTIL), Center for Computer Vision and Imaging Biomarkers, David Geffen School of Medicine, University of California Los Angeles, Los Angeles, CA

[4]Department of Radiological Sciences, David Geffen School of Medicine, University of California Los Angeles, Los Angeles, CA

[5]Department of Molecular and Medical Pharmacology, David Geffen School of Medicine, University of California Los Angeles, Los Angeles, CA

Abstract

Introduction—To report the potential value of pre-operative ^{18}F-FDOPA PET and anatomic MRI in diagnosis and prognosis of glioma patients.

Methods—Forty-five patients with a pathological diagnosis of glioma with pre-operative ^{18}F-FDOPA PET and anatomic MRI were retrospectively examined. The volume of contrast enhancement and T2 hyperintensity on MRI images along with the ratio of maximum ^{18}F-FDOPA SUV in tumor to normal tissue (T/N SUV_{max}) were measured and used to predict tumor grade, molecular status, and overall survival (OS).

Results—A significant correlation was observed between WHO grade and: the volume of contrast enhancement (r=0.67), volume of T2 hyperintensity (r=0.42), and ^{18}F-FDOPA uptake (r=0.60)($P < 0.01$ for each correlation). The volume of contrast enhancement and ^{18}F-FDOPA T/N SUV_{max} were significantly higher in glioblastoma (WHO IV) compared with lower grade gliomas

[#]Corresponding Author contact information: Benjamin M. Ellingson, Ph.D., Associate Professor of Radiology, Biomedical Physics, Psychiatry, and Bioengineering, Director, UCLA Brain Tumor Imaging Laboratory (BTIL), Departments of Radiological Sciences and Psychiatry, David Geffen School of Medicine, University of California, Los Angeles, 924 Westwood Blvd., Suite 615, Los Angeles, CA 90024 (bellingson@mednet.ucla.edu), Phone: (310) 481-7572, Fax: (310) 794-2796.

[*]Equal contribution

(WHO I–III), as well as for high-grade gliomas (WHO III–IV) compared with low-grade gliomas (WHO I–II). Receiver-operator characteristic (ROC) analyses confirmed the volume of contrast enhancement and ^{18}F-FDOPA T/N SUV_{max} could each differentiate patient groups. No significant differences in ^{18}F-FDOPA uptake were observed by IDH or MGMT status. Multivariable Cox regression suggested age (HR = 1.16, P = 0.0001) and continuous measures of ^{18}F-FDOPA PET T/N SUV_{max} (HR = 4.43, P = 0.016) were significant prognostic factors for OS in WHO I–IV gliomas.

Conclusions—Current findings suggest a potential role for the use of pre-operative ^{18}F-FDOPA PET in suspected glioma. Increased ^{18}F-FDOPA uptake may not only predict higher glioma grade, but also worse OS.

Keywords

^{18}F-FDOPA PET; biomarker; glioma; MRI

INTRODUCTION

Gliomas are the most common primary brain tumors in adults, and the survival rates for patients with glioblastoma (GBM) have remained grim for decades. According to the Central Brain Tumor Registry of the United States, the 1995–2012 survival rates for patients with GBM were 37.2% and 5.1% at 1-year and 5-years after diagnosis, respectively [1], and median survival for GBM is approximately 12–16 months [2–4]. At initial presentation, contrast-enhancement (CE) on the magnetic resonance imaging (MRI) scan, the gold standard for diagnosis and response assessment in malignant gliomas [5], may suggest a high-grade glioma (HGG), and up to 51% of newly-diagnosed GBMs may contain non-enhancing cortical signal abnormality [6]. In a prospective study of 53 newly-diagnosed brain tumor patients with non-CE lesions on MRI, 34% were found to have histologically-proven high-grade glioma [7].

The use of positron emission tomography (PET) molecular imaging can provide metabolic information that can complement MRI in questionable lesions. In 2016, the Response Assessment in Neuro-Oncology (RANO) working group and European Association for Neuro-Oncology (EANO) emphasized amino acid PET as a critically important imaging tool for diagnosis, response assessment, and clinical management of glioma patients [8]. Compared to traditional FDG PET, which maintains high uptake in normal neural tissues, amino acid PET tracers including methyl-L-[^{11}C]-methionine (^{11}C-MET), [^{18}F]-fluoro-ethyl-tyrosine (^{18}F-FET), and 3,4-dihydroxy-6-[^{18}F]-fluoro-L-phenylalanine (^{18}F-FDOPA) exhibit high tumor-to-background ratios and have exquisite specificity for identifying areas of active tumor [9–16]. The high level of amino acid uptake is in part due to the unique metabolic characteristics of cancer cells, which utilize neutral amino acids for fuel, cellular maintenance, and a variety of enzymatic processes. While ^{18}F-FET PET is a preferred radiotracer in much of the world including Europe and Australia due to its long half-life and relatively simple synthesis [16], ^{18}F-FDOPA PET is gaining traction because of its regular clinical use in the diagnosis of movement disorders. ^{18}F-FDOPA PET/CT has been shown to change the intended management of 41% of patients with brain tumors [17]. When used together, ^{18}F-FDOPA PET and MRI are believed to provide superior ability to diagnose [7],

predict the degree of malignancy, improve stereotactic guidance for biopsies, and differentiate pseudoprogression from true tumor progression in brain tumors [18–20].

Although some studies have examined ^{18}F-FDOPA PET characteristics in treatment-naïve glioma [7, 12, 19–30], few have examined ^{18}F-FDOPA PET combined with anatomic MRI features and even fewer have evaluated their ability to predict overall survival (OS). Such experience, even in small cohorts, is important to better understand the potential to change clinical decisions including treatment strategies. Thus, the purpose of the current retrospective study was to report our experience using ^{18}F-FDOPA PET and MRI in preoperative, treatment-naïve patients with suspected glioma with regards to differences in diagnosis and prognosis.

METHODS

Patient Selection

The UCLA Medical Center institutional review board approved this study (IRB IRB#15-000467). Consecutive patients from 2003 to 2016 with suspected glioma who underwent ^{18}F-FDOPA PET scan prior to biopsy or resection, radiation therapy, and chemotherapy were eligible for inclusion. A total of 73 consecutive scans were identified as being pre-intervention (e.g. prior to biopsy, resection, radiation therapy, and chemotherapy). Ten scans were excluded due to sequences with unusable radiotracer dose/timing header information (n=2), unavailability in the archival system (n=4), patients receiving carbidopa prior to the scan (n=2) [29], and lack of a post-scan tissue biopsy in patients who had a seizure (n=2). Thus, 63 upfront ^{18}F-FDOPA PET scans were identified in 59 unique patients. Of the 59 suspected glioma patients whose ^{18}F-FDOPA PET scans were initially identified, 45 patients had confirmed gliomas and available pre-operative anatomic MRI including post-contrast T1-weighted images and either T2-weighted turbo spin echo or T2-weighted fluid-attenuated inversion recovery (FLAIR) images. Of these patients, the mean age was 46.4±16.2 years and 51% were female. The distribution of World Health Organization (WHO) grade I (ganglioglioma), II, III, and IV gliomas was 4.4%, 35.6%, 31.1%, and 28.9%, respectively. OS was measured as the time interval from pathology-proven diagnosis until death or the last known alive time on the censor date (August 31, 2017). When available, isocitrate dehydrogenase 1/2 (IDH1/2) mutational status, 1p19q deletion status, and O^6-methylguanine–DNA methyltransferase (MGMT) promoter methylation results were obtained from the patient's clinical chart. Table 1 summarizes these patient demographics and glioma molecular status.

Magnetic Resonance Imaging Acquisition and Analysis

Anatomic MRI consisted of at least standard anatomic T1-weighted pre- and post-contrast images (2D axial turbo spin echo with 3 mm slice thickness and no interslice gap or 3D inversion-prepared gradient echo images with 1–1.5 mm isotropic voxel size), and 2D axial T2-weighted or T2-weighted FLAIR images acquired at 3 mm slice thickness with no interslice gap. The presence or absence of nodular CE on post-contrast T1-weighted images within the lesion was determined by the official clinical radiology report. A total of 23 of 45 patients (51%) lacked CE on post-contrast T1-weighted images.

Two regions of interests (ROI) were segmented by a single investigator (A.C.) and confirmed by another investigator (B.E.) using a semi-automatic procedure documented previously [31–33] and the Analysis of Functional NeuroImages (AFNI) software (NIMH Scientific and Statistical Computing Core; Bethesda, MD, USA). These investigators were blinded to the PET data and survival results. These regions of interest comprised 1) CE tumor from post-contrast T1-weighted images and 2) regions of T2 hyperintensity on T2-weighted or T2-weighted FLAIR images. For the segmentation of CE and T2 ROIs, a semi-automatic method was employed in which a large ROI was drawn over both CE regions on the post-contrast T1-weighted images (including necrosis) and T2 hyperintensities on the T2 or FLAIR images (i.e. non-CE tumor plus edema). Then, an intensity threshold was manually chosen to extract the CE tumor, plus any CE central necrosis, from the post-contrast T1-weighted images. Similarly, regions of T2 hyperintensity were segmented with manual thresholds on the T2 or FLAIR images, including areas of CE. All volumes are reported in cubic centimeters (cc).

^{18}F-FDOPA PET Image Acquisition and Analysis

^{18}F-FDOPA PET scans were acquired for all patients using a high-resolution full-ring PET scanner (ECAT-HR; CTI/MIMVista). Patients were instructed to fast for more than 4 h prior to PET acquisition. ^{18}F-FDOPA was synthesized and injected intravenously. A CT scan was acquired prior to PET for attenuation correction. Three-dimensional ^{18}F-FDOPA emission data were acquired for a total of 30 min. Data were integrated between 10 and 30 min from injection to obtain 20-min static ^{18}F-FDOPA images following reconstruction. PET images were reconstructed using an ordered-subset expectation maximization (OSEM) iterative reconstruction algorithm consisting of six iterations with eight subsets [34, 35]. Lastly, a Gaussian filter with a full width at half maximum of 4 mm was applied. The resulting voxel sizes were 1.34 mm × 1.34 mm × 3 mm for ^{18}F-FDOPA PET standard uptake volume (SUV) maps.

A 1 cm diameter spherical region of interest (ROI) analysis at the suspected tumor site (T) and contralateral normal-appearing white matter at the level of the centrum semiovale (NAWM) was performed on ^{18}F-FDOPA PET scans to calculate the quantitative measure of the metabolic activity of the radiotracer (SUV in g/mL) using the standard body weight method as previously reported [19]. The ratio of maximum SUV within the tumor to maximum SUV in NAWM was calculated (T/N SUV_{max}) and used for subsequent analyses. This was first done in a blinded fashion (without using lesion location information from the MRI scan), followed by an unblinded fashion in which the ROI was centered in the region of maximum ^{18}F-FDOPA uptake within the lesion as defined by the preoperative CE MRI closest in time to the ^{18}F-FDOPA scan. In cases of non-CE lesions, the T2-weighted MRI scan was used to guide the placement of the tumor ROI on the ^{18}F-FDOPA PET scan during the unblinded analysis.

Receiver Operator Characteristic (ROC) Analysis

The receiver operating characteristic (ROC) curve was used to determine whether the volume of CE, volume of T2 hyperintensity, and/or ^{18}F-FDOPA PET T/N SUV_{max} ratio could discriminate between either (a) GBM (WHO IV) and lower grade gliomas (WHO I–

III) and (b) high-grade gliomas (HGGs; WHO III–IV) from WHO I–II gliomas. The area under the curve (AUC) of each of the resulting ROC curves was further used to discriminate the outcomes.

Statistical Analyses

Statistical analysis was performed in Intercooled Stata version 9.2 (Stata Corp., College Station, TX) or Prism (Version 7.0c; GraphPad Software, La Jolla, CA). The Shapiro-Wilk test was used to test for normally-distributed data. For normally-distributed data, Student's t-test or analysis of variance (ANOVA) was performed. For non-normally-distributed data, a Mann-Whitney or Wilcoxon rank-sum analysis of medians was performed. Pearson or Spearman correlation coefficients were used to assess correlations between MRI measurements, ^{18}F-FDOPA PET T/N SUV_{max} ratio, and tumor grade. For AUC analysis of the ROC curves, logistic regression was used. Multivariable Cox regression was used to determine whether clinical covariates and continuous values of imaging measurements were significant predictors of OS. Kaplan-Meier curves were used to display differences in OS, and the log-rank test was used to compare survival when appropriate. Statistical significance was defined as alpha = 0.05. Bonferroni correction was used for multiple comparisons, resulting in a required level of significance of $P < 0.017$. Results are presented as percentage, mean±standard deviation, median with interquartile range (IQR), or range.

RESULTS

In general, the volume of CE, volume of T2 hyperintensity, and ^{18}F-FDOPA PET T/N SUV_{max} ratio increased with increasing glioma grade (Fig 1). Spearman rank correlation confirmed this general observation, showing a strong and significant correlation between the volume of CE and WHO grade (*r = 0.67, P < 0.00001*), volume of T2 hyperintensity and WHO grade (*r = 0.42, P = 0.0041*), and ^{18}F-FDOPA T/N SUV_{max} and WHO grade (*r = 0.60, P < 0.00001*). Pearson analysis revealed that the volume of CE and ^{18}F-FDOPA T/N SUV_{max} demonstrated a strong positive linear correlation (*r = 0.65, P < 0.00001*) across patients, but no such association was observed between the volume of T2 hyperintensity and ^{18}F-FDOPA T/N SUV_{max} (*r = 0.08, P = 0.59*), or between the volumes of CE and T2 hyperintensity (*r = 0.22, P = 0.16*).

The volume of CE (Fig 2A; 7.5±6.3 cc vs. 0.2±0.3 cc, *Mann-Whitney, P < 0.00001*) and ^{18}F-FDOPA PET T/N SUV_{max} (Fig 2C; 2.7±0.9 vs. 1.5±0.5, *P = 0.0002*), but not the volume of T2 hyperintensity (Fig 2B; 47.0±36.0 cc vs. 32.8±50.7 cc, *P = 0.04*), were significantly higher in GBM (WHO IV) gliomas compared to lower grade gliomas (WHO I–III), respectively, after Bonferroni correction. Similarly, ROC analysis indicated that the volume of contrast enhancement (*AUC = 0.95±0.05, P < 0.00001*) and ^{18}F-FDOPA PET T/N SUV_{max} (*AUC = 0.86±0.06, P < 0.00001*), but not the volume of T2 hyperintensity (*ROC AUC = 0.70±0.08, P = 0.37*), could differentiate GBM from WHO I–III gliomas with high sensitivity and specificity (Fig 2D). A volume of contrast enhancement larger than 1.2 cc had a 92% sensitivity and 100% specificity, and an ^{18}F-FDOPA PET T/N $SUV_{max} > 1.8$ had a sensitivity of 85% and specificity of 78%, in differentiating GBM from lower grade (WHO I–III) gliomas.

Likewise to the previous analysis, the volume of CE (Fig 2E; 3.7±5.7 cc vs. 0.1±0.3 cc, *Mann-Whitney, P < 0.00001*) and ^{18}F-FDOPA PET T/N SUV_{max} (Fig 2G; *Mann-Whitney,* 2.2±0.9 vs. 1.4±0.4, *P = 0.0002*), but not the volume of T2 hyperintensity (Fig 2F; 44.5±50.1 cc vs. 25.6±40.4 cc, *Mann-Whitney, P = 0.04*), were significantly higher in HGG (WHO III–IV) compared to low-grade glioma (LGG, WHO I–II), respectively, after Bonferroni correction. ROC analysis (Fig 2H) indicated that ^{18}F-FDOPA PET T/N SUV_{max} (*AUC = 0.86±0.06, P < 0.00001*) and the volume of contrast enhancement (*AUC = 0.95±0.05, P < 0.00001*) could significantly differentiate HGG from LGG, but the volume of T2 hyperintensity could not (*AUC = 0.70±0.09, P = 0.37*). Notably, the volume of contrast enhancement appeared to have high sensitivity and the volume of T2 hyperintensity had a high specificity for differentiating HGG from LGG, while ^{18}F-FDOPA PET T/N SUV_{max} had a balance of high sensitivity and specificity (T/N SUV_{max} > 1.7 [median value] had a 70% sensitivity and 78% specificity for differentiating HGG from LGG).

Among the 39 patients with available IDH mutation status, the volume of CE was significantly higher (Fig 3A; 3.5±4.9 cc vs. 0.1±0.3 cc, *Mann-Whitney, P = 0.0001*) in IDH wild-type compared with IDH mutant gliomas, respectively; however, no difference in the volume of T2 hyperintensity (Fig 3B; 33.0±30.8 cc vs. 47.7±64.9 cc, *P = 0.84*) or ^{18}F-FDOPA PET T/N SUV_{max} (Fig 3C; 2.2±0.9 vs. 1.5±0.5, *P = 0.022*) was observed after Bonferroni correction, respectively, although IDH wild-type tumors tended to have a higher ^{18}F-FDOPA uptake. Among the 33 patients with available MGMT promoter methylation status, no detectable difference in CE volume (Fig 3D; 3.0±5.0 cc vs. 1.7±4.0 cc, *Mann-Whitney, P = 0.37*), volume of T2 hyperintensity (Fig 3E; 40.4±62.2 cc vs. 45.6±39.6 cc, *P = 0.12*), or ^{18}F-FDOPA PET T/N SUV_{max} (Fig 3F; 2.0±1.0 vs. 1.8±0.9, *P = 0.66*) was observed between MGMT promoter methylated and unmethylated gliomas, respectively.

Multivariable Cox regression including age, WHO grade, volume of CE, volume of T2 hyperintensity, and ^{18}F-FDOPA PET T/N SUV_{max} ratio indicated that age (*hazard ratio [HR] = 1.16, P=0.0001*) and ^{18}F-FDOPA PET T/N SUV_{max} (*HR = 4.43, P = 0.016*) were significant independent predictors of OS (Table 2). Identification of “high-risk” glioma patients (n=14) as patients having both a volume of MRI CE greater than 1 cc (i.e. “measurable” tumor) and ^{18}F-FDOPA PET T/N SUV_{max} greater than 1.7 (group median) resulted in a significantly shorter survival compared with all other glioma patients (Fig 4; *log-rank, HR = 3.05, P = 0.012*).

During the blinded analysis of the ^{18}F-FDOPA scans, the region of maximum ^{18}F-FDOPA uptake in the entire extrastriatal brain was determined without using lesion location information from the corresponding MRI scan. Interestingly, we observed significant uptake in the posterior fossa, particularly the cerebellum and midbrain, which exhibited the highest ^{18}F-FDOPA SUV_{max} among all extrastriatal brain regions in 9 of the cases (20%) analyzed. Among the patients whose blinded and unblinded tumor ROIs (based on ^{18}F-FDOPA SUV_{max}) did not co-localize (n=11 total, the additional two cases included maximum uptake in the right occipital lobe [in a patient with a right frontal lobe grade II glioma] and superior frontal gyrus [in a patient with a left parietal grade III glioma]), four went on to have recurrent glioma. However, tumor recurrence did not occur in the region of maximum ^{18}F-FDOPA uptake on blinded analysis (i.e. the non-co-localizing region).

DISCUSSION

Previous studies in recurrent glioma have used similar techniques to determine the predictive capability of a T/N SUV ratio threshold in delineating HGG from LGG [19, 21], while others evaluated the lesion SUV alone (mean or maximum) [27] or rate constants calculated from dynamic ^{18}F-FDOPA PET scans [29]. In the current study we showed that the T/N SUV_{max} ratio greater than 1.7 (series median) could best differentiate HGG from other lesions, which is slightly lower than prior studies [18, 20, 26]. Fueger *et al.* studied upfront ^{18}F-FDOPA PET in 22 newly-diagnosed glioma cases, reporting a significant difference in SUV_{max} in tumor alone among grade II, III, and IV gliomas, and that a SUV_{max} within the tumor greater than 2.72 discriminated HGG vs. LGG with a sensitivity of 85% and a specificity of 89% [19]. This is comparable to the work of Pafundi *et al.* in a small cohort of newly-diagnosed glioma cases, which showed that a T/N SUV_{max} ratio threshold of 2 delineated between HGG and LGG [21]. In a study of 20 newly-diagnosed glioma cases, Nioche *et al.* similarly reported that an upfront tumor SUV_{mean} threshold of 2.5 could distinguish HGG vs. LGG with a sensitivity of 70% and a specificity of 90% [27].

In a prospective study of 16 glioma patients with <10% MRI CE tumor volume who also underwent preoperative 11C-methionine PET and 18F-FDG PET, the tissue from lesions positive for CE, T2 hyperintensity, 11C-methionine signal, and 18F-FDG signal gave an accurate diagnosis of grade in only 40% of cases [36]. Taken together with previous investigations[6, 7], these studies highlight the diagnostic dilemma of determining high-grade glioma based on MRI alone, or in combination with 11C-methionine PET and 18F-FDG PET, in the newly-diagnosed setting. Results from the current study suggest combined information from both MRI and ^{18}F-FDOPA PET may improve this prediction. This finding is similar to Bund e*t al.*, who reported a tumor to normal brain SUV_{max} ratio larger than 2.16 could differentiate between non-CE HGG and non-CE LGG with a sensitivity and specificity of 60% and 100%, respectively [7]. As lower grade diffuse glioma patients are more often monitored prior to initial therapeutic interventions, the current study suggestions ^{18}F-FDOPA PET in patients lacking contrast enhancement may increase the ability to detect HGG, which may expedite effective treatment.

The absence of a significant difference in the ^{18}F-FDOPA T/N SUV_{max} ratio based on IDH mutational status and MGMT promoter methylation status is the second report of such an attempt at correlating ^{18}F-FDOPA uptake with these molecular subtypes of glioma. Although not significant, it is notable the T/N SUV_{max} ratio was elevated within IDH wild type tumors compared with IDH mutant tumors. Verger and colleagues retrospectively analyzed preoperative ^{18}F-FDOPA uptake in 43 treatment-naïve grade II/III glioma patients and found a significantly higher T/N SUV_{max} ratio in IDH-mutated compared to wild-type tumors [37]. Further studies are needed to confirm these observations, as well as the exploration of ^{18}F-FDOPA uptake among patients with other molecular markers including TP53 mutations and loss of heterozygosity of 1p and 19q.

Results from the current study suggest the ^{18}F-FDOPA PET T/N SUV_{max} ratio may be a significant independent predictor of OS in glioma patients, regardless of tumor grade or lesion size. Although previous studies have indicated that enhancing tumor volume was

predictive of OS [5, 31], this evidence appears to be largely restricted to malignant gliomas including GBM and may not extend to lower grade gliomas as indicated by the lack of correlation with OS in the current study. However, when MRI features of contrast enhancement were combined with ^{18}F-FDOPA PET uptake, high-risk glioma patients had approximately three times shorter overall survival compared to that of all other patients.

Study Limitations

The findings of this study should be interpreted in the context of its limitations. The retrospective nature of the study did not allow for the control of potential confounding variables in the analysis (e.g. physician biases regarding when to order the ^{18}F-FDOPA scan). Additionally, the use of SUV_{max} within the tumor region instead of strictly examining the distribution in MR-defined regions (e.g. CE or T2/FLAIR hyperintense regions) was a potential limitation, but was chosen based on similar approaches [19, 21] and the ease of rapid evaluation in clinical contexts.

The highest ^{18}F-FDOPA extrastriatal uptake was noticed outside of the MRI-based tumor region in 11 cases (24.4%) during the blinded analysis, and 9 of these instances occurred in the posterior fossa in normal brain tissue. This may represent a pattern of normal brain biodistribution of ^{18}F-FDOPA uptake. The reasons for this finding of increased ^{18}F-FDOPA uptake in the posterior fossa despite absence of glioma remain unclear. Previous studies in canine [38] and rodent [39] brain have identified expression of the L-type amino acid transporter 1 (LAT1, the primary transporter responsible for ^{18}F-FDOPA uptake in the brain) in the cerebellum, which is found to correlate with ^{18}F-FDOPA uptake [40]. The fact that no recurrences occurred in the non-co-localizing regions (predominantly posterior fossa) suggests that high ^{18}F-FDOPA uptake in the posterior fossa should not pose a clinical concern if the suspected glioma is outside of the posterior fossa based on MRI.

Future prospective studies evaluating the utility of upfront ^{18}F-FDOPA in suspected newly-diagnosed glioma [20] could consider standardizing the time window between the upfront ^{18}F-FDOPA PET scan and the biopsy/resection, time between radiotracer injection and image acquisition, and integrating the ^{18}F-FDOPA PET scan data into the neurosurgical navigation software to ensure optimal tissue sampling. Wider adoption of upfront ^{18}F-FDOPA PET scans in suspected glioma will depend on their utility in clinical decision-making, the number-needed-to-scan to avoid an unnecessary biopsy/resection, and their ability to predict OS.

CONCLUSION

In conclusion, current findings suggest a role for the use of preoperative ^{18}F-FDOPA PET in suspected glioma. Increased ^{18}F-FDOPA uptake not only predicted higher tumor grade, but also worse outcome. In combination with contrast-enhanced MRI, ^{18}F-FDOPA PET identified a subgroup of high-risk patients whose OS was one-third the OS of all other patients. Prospective studies are needed to validate these observations and to determine the impact of routine preoperative implementation of ^{18}F-FDOPA PET scanning combined with MRI in clinical decision-making, cost of care, and patient outcomes.

Acknowledgments

Funding Sources

NIH/NINDS R25 NS065723 Translational Neuroscience Training Grant (Patel); American Medical Association Foundation Seed Research Grant (Patel); American Cancer Society (ACS) Research Scholar Grant (RSG-15-003-01-CCE) (Ellingson); American Brain Tumor Association (ABTA) Research Collaborators Grant (ARC1700002)(Ellingson); National Brain Tumor Society (NBTS) Research Grant (Ellingson, Cloughesy); Art of the Brain (Cloughesy); NIH/NCI UCLA Brain Tumor SPORE (1P50CA211015-01A1) (Ellingson, Lai, Cloughesy, Nghiemphu); NIH/NCI 1R21CA223757-01 (Ellingson)

References

1. Ostrom QT, Gittleman H, Fulop J, Liu M, Blanda R, Kromer C, Wolinsky Y, Kruchko C, Barnholtz-Sloan JS. CBTRUS Statistical Report: Primary Brain and Central Nervous System Tumors Diagnosed in the United States in 2008–2012. Neuro Oncol. 2015; 17(Suppl 4):iv1–iv62. [PubMed: 26511214]
2. Stupp R, Taillibert S, Kanner AA, Kesari S, Steinberg DM, Toms SA, Taylor LP, Lieberman F, Silvani A, Fink KL, Barnett GH, Zhu JJ, Henson JW, Engelhard HH, Chen TC, Tran DD, Sroubek J, Tran ND, Hottinger AF, Landolfi J, Desai R, Caroli M, Kew Y, Honnorat J, Idbaih A, Kirson ED, Weinberg U, Palti Y, Hegi ME, Ram Z. Maintenance Therapy With Tumor-Treating Fields Plus Temozolomide vs Temozolomide Alone for Glioblastoma: A Randomized Clinical Trial. JAMA. 2015; 314:2535–2543. [PubMed: 26670971]
3. Chinot OL, Nishikawa R, Mason W, Henriksson R, Saran F, Cloughesy T, Garcia J, Revil C, Abrey L, Wick W. Upfront bevacizumab may extend survival for glioblastoma patients who do not receive second-line therapy: an exploratory analysis of AVAglio. Neuro Oncol. 2016; 18:1313–1318. [PubMed: 27006178]
4. Stupp R, Taillibert S, Kanner A, Read W, Steinberg DM, Lhermitte B, Toms S, Idbaih A, Ahluwalia MS, Fink K, Di Meco F, Lieberman F, Zhu JJ, Stragliotto G, Tran DD, Brem S, Hottinger AF, Kirson ED, Lavy-Shahaf G, Weinberg U, Kim CY, Paek SH, Nicholas G, Burna J, Hirte H, Weller M, Palti Y, Hegi ME, Ram Z. Effect of Tumor-Treating Fields Plus Maintenance Temozolomide vs Maintenance Temozolomide Alone on Survival in Patients With Glioblastoma: A Randomized Clinical Trial. JAMA. 2017; 318:2306–2316. [PubMed: 29260225]
5. Ellingson BM, Wen PY, Cloughesy TF. Evidence and Context of Use for Contrast Enhancement as a Surrogate of Disease Burden and Treatment Response in Malignant Glioma. Neuro Oncol. 2017
6. Lasocki A, Gaillard F, Tacey M, Drummond K, Stuckey S. Incidence and prognostic significance of non-enhancing cortical signal abnormality in glioblastoma. J Med Imaging Radiat Oncol. 2016; 60:66–73. [PubMed: 26597591]
7. Bund C, Heimburger C, Imperiale A, Lhermitte B, Chenard MP, Lefebvre F, Kremer S, Proust F, Namer IJ. FDOPA PET-CT of Nonenhancing Brain Tumors. Clin Nucl Med. 2017; 42:250–257. [PubMed: 28114224]
8. Albert NL, Weller M, Suchorska B, Galldiks N, Soffietti R, Kim MM, la Fougere C, Pope W, Law I, Arbizu J, Chamberlain MC, Vogelbaum M, Ellingson BM, Tonn JC. Response Assessment in Neuro-Oncology working group and European Association for Neuro-Oncology recommendations for the clinical use of PET imaging in gliomas. Neuro Oncol. 2016; 18:1199–1208. [PubMed: 27106405]
9. Ullrich RT, Kracht L, Brunn A, Herholz K, Frommolt P, Miletic H, Deckert M, Heiss WD, Jacobs AH. Methyl-L-11C-methionine PET as a diagnostic marker for malignant progression in patients with glioma. J Nucl Med. 2009; 50:1962–1968. [PubMed: 19910435]
10. Singhal T, Narayanan TK, Jacobs MP, Bal C, Mantil JC. 11C-methionine PET for grading and prognostication in gliomas: a comparison study with 18F-FDG PET and contrast enhancement on MRI. J Nucl Med. 2012; 53:1709–1715. [PubMed: 23055534]
11. Nihashi T, Dahabreh IJ, Terasawa T. Diagnostic accuracy of PET for recurrent glioma diagnosis: a meta-analysis. AJNR Am J Neuroradiol. 2013; 34:944–950. S941–911. [PubMed: 23124638]

12. Chen W, Silverman DH, Delaloye S, Czernin J, Kamdar N, Pope W, Satyamurthy N, Schiepers C, Cloughesy T. 18F-FDOPA PET imaging of brain tumors: comparison study with 18F-FDG PET and evaluation of diagnostic accuracy. J Nucl Med. 2006; 47:904–911. [PubMed: 16741298]
13. Popperl G, Kreth FW, Mehrkens JH, Herms J, Seelos K, Koch W, Gildehaus FJ, Kretzschmar HA, Tonn JC, Tatsch K. FET PET for the evaluation of untreated gliomas: correlation of FET uptake and uptake kinetics with tumour grading. Eur J Nucl Med Mol Imaging. 2007; 34:1933–1942. [PubMed: 17763848]
14. Calcagni ML, Galli G, Giordano A, Taralli S, Anile C, Niesen A, Baum RP. Dynamic O-(2-[18F]fluoroethyl)-L-tyrosine (F-18 FET) PET for glioma grading: assessment of individual probability of malignancy. Clin Nucl Med. 2011; 36:841–847. [PubMed: 21892031]
15. Rapp M, Heinzel A, Galldiks N, Stoffels G, Felsberg J, Ewelt C, Sabel M, Steiger HJ, Reifenberger G, Beez T, Coenen HH, Floeth FW, Langen KJ. Diagnostic performance of 18F-FET PET in newly diagnosed cerebral lesions suggestive of glioma. J Nucl Med. 2013; 54:229–235. [PubMed: 23232275]
16. Dunet V, Rossier C, Buck A, Stupp R, Prior JO. Performance of 18F-fluoro-ethyl-tyrosine (18F-FET) PET for the differential diagnosis of primary brain tumor: a systematic review and Metaanalysis. J Nucl Med. 2012; 53:207–214. [PubMed: 22302961]
17. Walter F, Cloughesy T, Walter MA, Lai A, Nghiemphu P, Wagle N, Fueger B, Satyamurthy N, Phelps ME, Czernin J. Impact of 3,4-dihydroxy-6-18F-fluoro-L-phenylalanine PET/CT on managing patients with brain tumors: the referring physician's perspective. J Nucl Med. 2012; 53:393–398. [PubMed: 22323780]
18. Bell C, Dowson N, Puttick S, Gal Y, Thomas P, Fay M, Smith J, Rose S. Increasing feasibility and utility of (18)F-FDOPA PET for the management of glioma. Nucl Med Biol. 2015; 42:788–795. [PubMed: 26162582]
19. Fueger BJ, Czernin J, Cloughesy T, Silverman DH, Geist CL, Walter MA, Schiepers C, Nghiemphu P, Lai A, Phelps ME, Chen W. Correlation of 6-18F-fluoro-L-dopa PET uptake with proliferation and tumor grade in newly diagnosed and recurrent gliomas. J Nucl Med. 2010; 51:1532–1538. [PubMed: 20847166]
20. Villani V, Carapella CM, Chiaravalloti A, Terrenato I, Piludu F, Vidiri A, Schillaci O, Floris R, Marzi S, Fabi A, Pace A. The Role of PET [18F]FDOPA in Evaluating Low-grade Glioma. Anticancer Res. 2015; 35:5117–5122. [PubMed: 26254416]
21. Pafundi DH, Laack NN, Youland RS, Parney IF, Lowe VJ, Giannini C, Kemp BJ, Grams MP, Morris JM, Hoover JM, Hu LS, Sarkaria JN, Brinkmann DH. Biopsy validation of 18F-DOPA PET and biodistribution in gliomas for neurosurgical planning and radiotherapy target delineation: results of a prospective pilot study. Neuro Oncol. 2013; 15:1058–1067. [PubMed: 23460322]
22. Heiss WD, Wienhard K, Wagner R, Lanfermann H, Thiel A, Herholz K, Pietrzyk U. F-Dopa as an amino acid tracer to detect brain tumors. J Nucl Med. 1996; 37:1180–1182. [PubMed: 8965194]
23. Dowson N, Thomas P, Fay M, Jeffree RL, Gal Y, Bourgeat P, Smith J, Winter C, Coulthard A, Salvado O, Crozier S, Rose S. Early prediction of treatment response in advanced gliomas with (18)F-dopa positron-emission tomography. Curr Oncol. 2014; 21:e172–178. [PubMed: 24523617]
24. Janvier L, Olivier P, Blonski M, Morel O, Vignaud JM, Karcher G, Taillandier L, Verger A. Correlation of SUV-Derived Indices With Tumoral Aggressiveness of Gliomas in Static 18F-FDOPA PET: Use in Clinical Practice. Clin Nucl Med. 2015; 40:e429–435. [PubMed: 26204212]
25. Lapa C, Linsenmann T, Monoranu CM, Samnick S, Buck AK, Bluemel C, Czernin J, Kessler AF, Homola GA, Ernestus RI, Lohr M, Herrmann K. Comparison of the amino acid tracers 18F-FET and 18F-DOPA in high-grade glioma patients. J Nucl Med. 2014; 55:1611–1616. [PubMed: 25125481]
26. Ledezma CJ, Chen W, Sai V, Freitas B, Cloughesy T, Czernin J, Pope W. 18F-FDOPA PET/MRI fusion in patients with primary/recurrent gliomas: initial experience. Eur J Radiol. 2009; 71:242–248. [PubMed: 18511228]
27. Nioche C, Soret M, Gontier E, Lahutte M, Dutertre G, Dulou R, Capelle L, Guillevin R, Foehrenbach H, Buvat I. Evaluation of quantitative criteria for glioma grading with static and dynamic 18F-FDopa PET/CT. Clin Nucl Med. 2013; 38:81–87. [PubMed: 23334119]

28. Rose S, Fay M, Thomas P, Bourgeat P, Dowson N, Salvado O, Gal Y, Coulthard A, Crozier S. Correlation of MRI-derived apparent diffusion coefficients in newly diagnosed gliomas with [18F]-fluoro-L-dopa PET: what are we really measuring with minimum ADC? AJNR Am J Neuroradiol. 2013; 34:758–764. [PubMed: 23079407]
29. Schiepers C, Chen W, Cloughesy T, Dahlbom M, Huang SC. 18F-FDOPA kinetics in brain tumors. J Nucl Med. 2007; 48:1651–1661. [PubMed: 17873130]
30. Tripathi M, Sharma R, D'Souza M, Jaimini A, Panwar P, Varshney R, Datta A, Kumar N, Garg G, Singh D, Grover RK, Mishra AK, Mondal A. Comparative evaluation of F-18 FDOPA, F-18 FDG, and F-18 FLT-PET/CT for metabolic imaging of low grade gliomas. Clin Nucl Med. 2009; 34:878–883. [PubMed: 20139821]
31. Ellingson BM, Harris RJ, Woodworth DC, Leu K, Zaw O, Mason WP, Sahebjam S, Abrey LE, Aftab DT, Schwab GM, Hessel C, Lai A, Nghiemphu PL, Pope WB, Wen PY, Cloughesy TF. Baseline pretreatment contrast enhancing tumor volume including central necrosis is a prognostic factor in recurrent glioblastoma: evidence from single and multicenter trials. Neuro Oncol. 2017; 19:89–98. [PubMed: 27580889]
32. Ellingson BM, Kim HJ, Woodworth DC, Pope WB, Cloughesy JN, Harris RJ, Lai A, Nghiemphu PL, Cloughesy TF. Recurrent glioblastoma treated with bevacizumab: contrast-enhanced T1-weighted subtraction maps improve tumor delineation and aid prediction of survival in a multicenter clinical trial. Radiology. 2014; 271:200–210. [PubMed: 24475840]
33. Tran AN, Lai A, Li S, Pope WB, Teixeira S, Harris RJ, Woodworth DC, Nghiemphu PL, Cloughesy TF, Ellingson BM. Increased sensitivity to radiochemotherapy in IDH1 mutant glioblastoma as demonstrated by serial quantitative MR volumetry. Neuro Oncol. 2014; 16:414–420. [PubMed: 24305712]
34. Kinahan PE, Townsend DW, Beyer T, Sashin D. Attenuation correction for a combined 3D PET/CT scanner. Med Phys. 1998; 25:2046–2053. [PubMed: 9800714]
35. Nuyts J, Michel C, Dupont P. Maximum-likelihood expectation-maximization reconstruction of sinograms with arbitrary noise distribution using NEC-transformations. IEEE Trans Med Imaging. 2001; 20:365–375. [PubMed: 11403196]
36. Ideguchi M, Nishizaki T, Ikeda N, Okamura T, Tanaka Y, Fujii N, Ohno M, Shimabukuro T, Kimura T, Ikeda E, Suga K. A surgical strategy using a fusion image constructed from 11C-methionine PET, 18F-FDG-PET and MRI for glioma with no or minimum contrast enhancement. J Neurooncol. 2018
37. Verger A, Metellus P, Sala Q, Colin C, Bialecki E, Taieb D, Chinot O, Figarella-Branger D, Guedj E. IDH mutation is paradoxically associated with higher (18)F-FDOPA PET uptake in diffuse grade II and grade III gliomas. Eur J Nucl Med Mol Imaging. 2017; 44:1306–1311. [PubMed: 28293705]
38. Ochiai H, Morishita T, Onda K, Sugiyama H, Maruo T. Canine Lat1: molecular structure, distribution and its expression in cancer samples. J Vet Med Sci. 2012; 74:917–922. [PubMed: 22322188]
39. Duelli R, Enerson BE, Gerhart DZ, Drewes LR. Expression of large amino acid transporter LAT1 in rat brain endothelium. J Cereb Blood Flow Metab. 2000; 20:1557–1562. [PubMed: 11083230]
40. Youland RS, Kitange GJ, Peterson TE, Pafundi DH, Ramiscal JA, Pokorny JL, Giannini C, Laack NN, Parney IF, Lowe VJ, Brinkmann DH, Sarkaria JN. The role of LAT1 in (18)F-DOPA uptake in malignant gliomas. J Neurooncol. 2013; 111:11–18. [PubMed: 23086431]

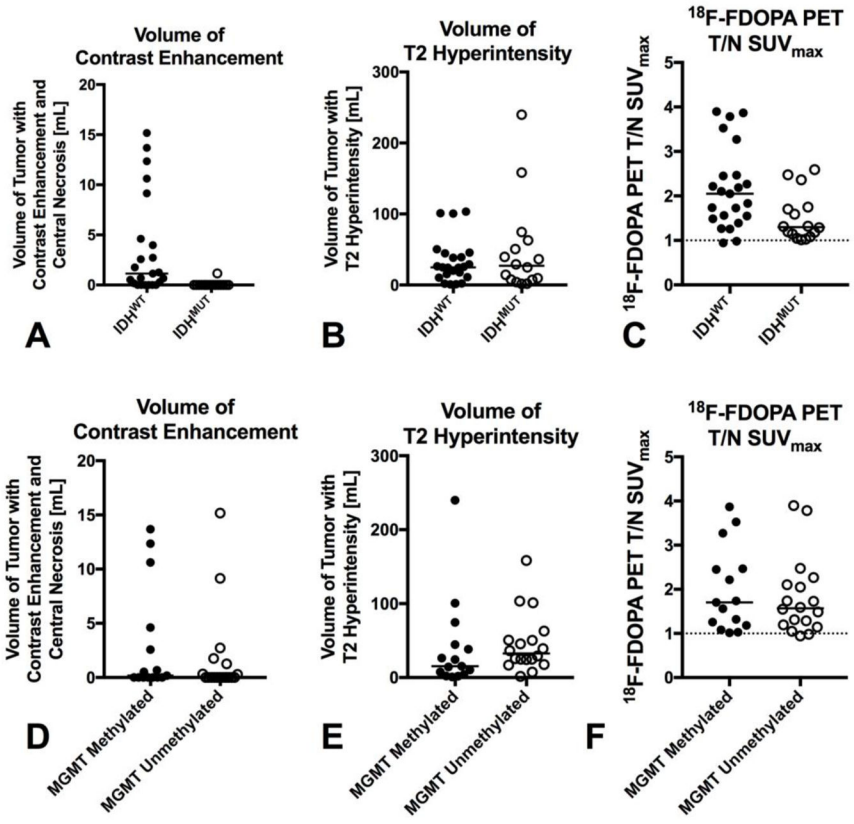

Fig. 1. Post-contrast T1-weighted images, T2-weighted turbo spin echo or fluid attenuated inversion recovery (FLAIR) images, and ^{18}F-FDOPA PET SUV maps for representative patients

A) 19-year-old female with a World Health Organization (WHO) grade I ganglioglioma. B) 24-year-old female with a WHO grade II diffuse astrocytoma. C) 32-year-old male with WHO grade III anaplastic oligodendroglioma. D) 74-year-old male with WHO IV glioblastoma.

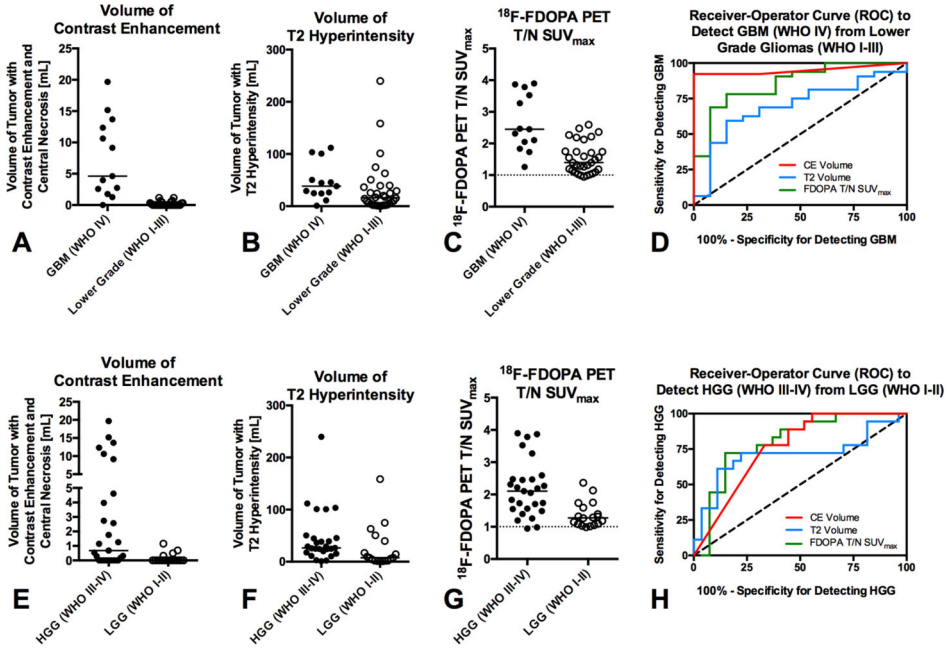

Fig. 2. Anatomic MRI and ^{18}F-FDOPA PET measurements in glioma patients

A) Volume of contrast enhancement, B) volume of T2 hyperintensity, and C) ^{18}F-FDOPA PET T/N SUV_{max} ratio comparisons between World Health Organization (WHO) IV glioblastoma (GBM) and lower grade gliomas (WHO I–III). D) Receiver-operator characteristic (ROC) curves illustrating sensitivity and specificity of anatomic MRI and ^{18}F-FDOPA PET measurements to differentiate WHO IV GBM from lower trade gliomas (WHO I–III). E) Volume of contrast enhancement, F) volume of T2 hyperintensity, and G) ^{18}F-FDOPA PET T/N SUV_{max} ratio comparisons between high-grade gliomas (HGG; WHO III–IV) and low-grade gliomas (LGG; WHO I–II). H) ROC curves illustrating sensitivity and specificity of anatomic MRI and ^{18}F-FDOPA PET measurements in discriminating HGG from LGG.

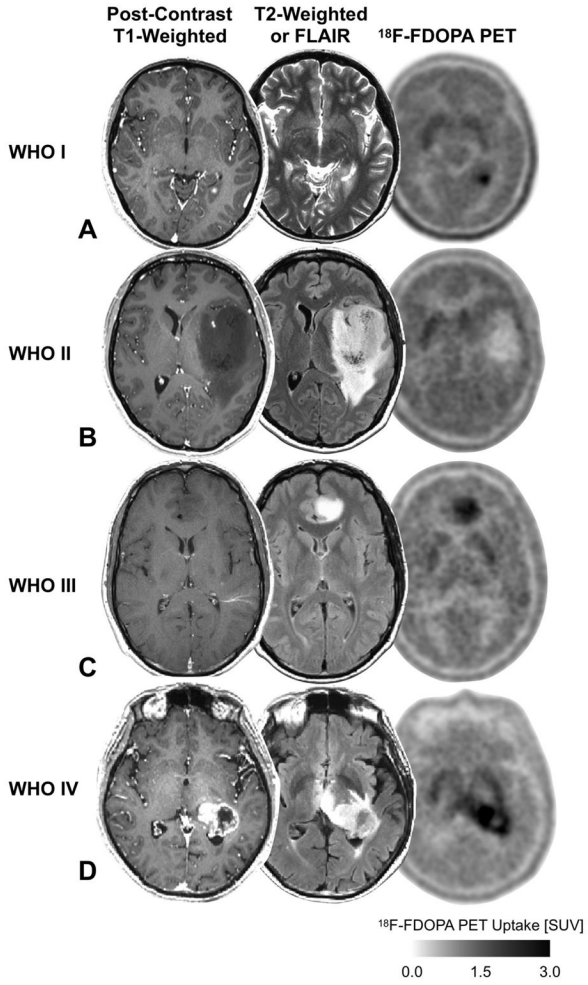

Fig. 3. Anatomic MRI and ^{18}F-FDOPA PET measurements across IDH mutation status and MGMT promoter methylation status

A) Volume of contrast enhancement, B) volume of T2 hyperintensity, and C) ^{18}F-FDOPA PET T/N SUV_{max} ratio comparisons between isocitrate dehydrogenase (IDH) mutant (IDH^{MUT}) and wild type (IDH^{WT}) gliomas (n=39 evaluable). D) Volume of contrast enhancement, E) volume of T2 hyperintensity, and F) ^{18}F-FDOPA PET T/N SUV_{max} ratio comparisons between O^6-methylguanine-DNA methyltransferase (MGMT) promoter methylated and unmethylated gliomas (n=33 evaluable).

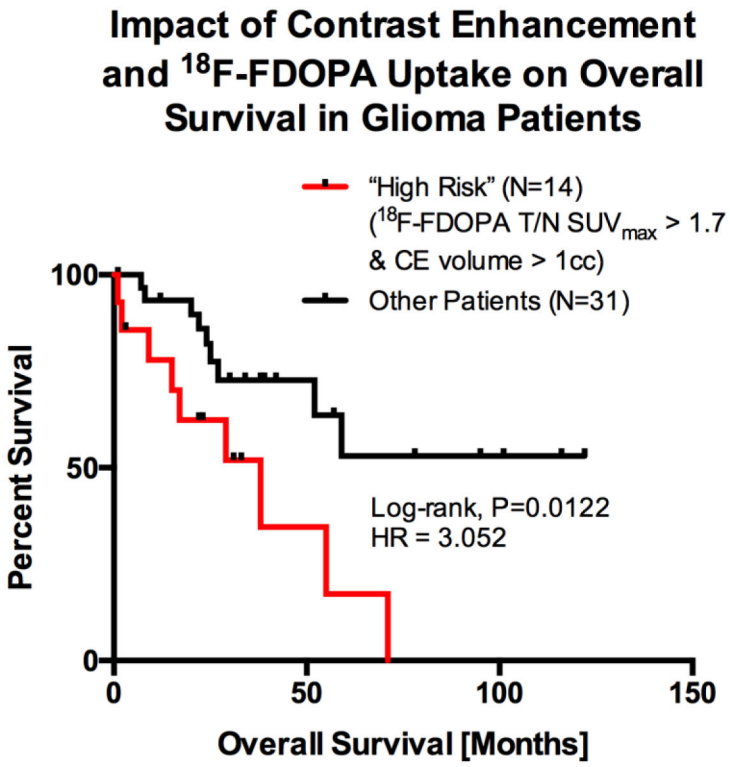

Fig. 4. Kaplan-Meier survival curves for composite MRI and ^{18}F-FDOPA PET index of high-risk glioma patients

High-risk patients (N=14) were defined as those with volume of contrast enhancement (CE) greater than 1 cc ("measurable tumor") and ^{18}F-FDOPA PET T/N SUV_{max} ratio greater than 1.7 (group median). Results demonstrate a significantly shorter OS in high high-risk patients (*Log-rank, HR = 3.05, P=0.012*).

Table 1

Patient Demographics.

Age (y)	Sex	MGMT Promoter Methylation Status	IDH 1/2 Mutation Status	WHO Grade	Pathological Diagnosis
43	Female	-	-	I	Ganglioglioma
19	Female	-	-	I	Ganglioglioma
57	Female	U	-	II	Astrocytoma
47	Male	U	MUT	II	Astrocytoma
63	Female	-	WT	II	Astrocytoma
36	Male	M	MUT	II	Astrocytoma
33	Male	M	MUT	II	Astrocytoma
24	Female	U	MUT	II	Astrocytoma
52	Male	-	MUT	II	Astrocytoma
33	Male	-	-	II	Oligodendroglioma
24	Male	U	MUT	II	Oligodendroglioma
29	Male	-	WT	II	Oligodendroglioma
27	Female	-	MUT	II	Oligodendroglioma
36	Male	M	MUT	II	Oligodendroglioma
61	Male	U	MUT	II	Oligodendroglioma
28	Female	U	MUT	II	Oligodendroglioma
47	Female	M	MUT	II	Oligodendroglioma
26	Female	M	MUT	II	Oligodendroglioma
18	Male	-	-	III	Anaplastic Astrocytoma
60	Male	U	WT	III	Anaplastic Astrocytoma
71	Male	U	WT	III	Anaplastic Astrocytoma
58	Male	U	WT	III	Anaplastic Astrocytoma
60	Female	M	WT	III	Anaplastic Astrocytoma
60	Female	M	WT	III	Anaplastic Astrocytoma
58	Female	U	WT	III	Anaplastic Astrocytoma
62	Female	-	WT	III	Anaplastic Astrocytoma
38	Male	M	MUT	III	Anaplastic Astrocytoma
68	Male	M	WT	III	Anaplastic Astrocytoma

Age (y)	Sex	MGMT Promoter Methylation Status	IDH 1/2 Mutation Status	WHO Grade	Pathological Diagnosis
25	Female	U	MUT	III	Anaplastic Oligoastrocytoma
35	Female	U	MUT	III	Anaplastic Oligodendroglioma
32	Male	-	MUT	III	Anaplastic Oligodendroglioma
53	Male	U	WT	III	Anaplastic Oligodendroglioma
60	Female	M	WT	IV	Glioblastoma
54	Female	M	WT	IV	Glioblastoma
47	Female	M	WT	IV	Glioblastoma
54	Male	M	WT	IV	Glioblastoma
64	Male	M	WT	IV	Glioblastoma
68	Male	-	WT	IV	Glioblastoma
26	Female	U	WT	IV	Glioblastoma
43	Female	U	WT	IV	Glioblastoma
38	Female	U	WT	IV	Glioblastoma
48	Female	-	-	IV	Glioblastoma
74	Male	M	WT	IV	Glioblastoma
54	Female	U	WT	IV	Glioblastoma
75	Male	U	WT	IV	Glioblastoma

-=Unknown, IDH=isocitrate dehydrogenase, M=Methylated, MGMT=O^6-methylguanine–DNA methyltransferase, MUT=Mutant, U=Unmethylated,, WHO=World Health Organization, WT=Wild Type. Age is at the time of diagnosis.

Table 2

Multivariable Cox Regression Results.

Variable	Coefficient	Hazard Ratio	95% C.I.	P-Value
Age	0.15±0.04	1.16	(1.07–1.25)	0.0001***
WHO Grade	0.19±0.42	1.20	(0.53–2.72)	0.66
Contrast Enhancing MRI Volume [cc] (Continuous)	−0.18±0.10	0.84	(0.69–1.02)	0.08
T2 Hyperintense MRI Volume [cc] (Continuous)	0.011±0.009	1.01	(0.99–1.03)	0.20
^{18}F-FDOPA PET T/N SUV_{max} Ratio (Continuous)	1.49±0.62	4.43	(1.32–14.85)	0.016*

*P<0.05,

***P<0.001